LETTERS
PUBLISHED ONLINE: 13 APRIL 2015 | DOI: 10.1038/NPHOTON.2015.61

nature photonics

Controllable spatiotemporal nonlinear effects in multimode fibres

Logan G. Wright[1]*, Demetrios N. Christodoulides[2] and Frank W. Wise[1]

Multimode fibres are of interest for next-generation telecommunications systems and the construction of high-energy fibre lasers. However, relatively little work has explored nonlinear pulse propagation in multimode fibres. Here, we consider highly nonlinear ultrashort pulse propagation in the anomalous-dispersion regime of a graded-index multimode fibre. Low modal dispersion and strong nonlinear coupling between the fibre's many spatial modes result in interesting behaviour. We observe spatiotemporal effects reminiscent of nonlinear optics in bulk media—self-focusing and multiple filamentation[1,2]—at a fraction of the usual power. By adjusting the spatial initial conditions, we generate on-demand, megawatt, ultrashort pulses tunable between 1,550 and 2,200 nm; dispersive waves over one octave; intense combs of visible light; and a multi-octave-spanning supercontinuum. Our results indicate that multimode fibres present unique opportunities for observing new spatiotemporal dynamics and phenomena. They also enable the realization of a new type of tunable, broadband fibre source that could be useful for many applications.

Multimode (MM) optical fibres are common, and even predate single-mode fibres (SMF). However, the high bandwidth and structural simplicity of SMF caused interest in multimode systems to wane by the early 1980s, and, as a result, their nonlinear properties have remained largely unexplored. Although a considerable body of theoretical work exists on highly-multimode nonlinear optics[3–8], there have been surprisingly few experimental studies (and all, including those described in refs 9–11, use long pulses in the normal dispersion regime). In nearly all experimental work with multimode fibres, a single mode (usually the lowest-order mode) is excited, with intermodal nonlinear effects involving at most only a few specific modes. Although they essentially explore perturbed one-dimensional propagation, these studies hint at the potential power of spatial degrees of freedom (for example, intermodal dispersion allows phase matching of intermodal four-wave mixing (FWM) or dispersive wave (DW) radiation processes[12–16]).

In this Letter we demonstrate and control novel spatiotemporal nonlinear dynamics in the highly nonlinear, strongly coupled, many-mode regime. In addition to the many effects that are related to those commonly observed in SMF-based supercontinuum generation, we observe spatial nonlinear processes that resemble those typically encountered in two- and three-dimensional nonlinear optics[1,2]. These are qualitatively new, however, and result from spatiotemporal soliton fissions and interactions. In contrast with previous work, we consider high-energy pulse propagation in the anomalous-dispersion regime of a graded-index (GRIN) fibre with low intermodal dispersion. In all cases, we deliberately launch light simultaneously into various distributions of many modes by adjusting the initial conditions (angle of launch, excitation radial position and phase front). By optimizing these conditions in real time, we demonstrate continuous control over many new effects and achieve on-demand, unprecedented performance from a fibre light source.

To determine the possible effects that can be observed at relevant energy levels, we conducted numerical simulations. Varying the initial spatial conditions in the theoretical model led to variations in the resulting propagation behaviour (Supplementary Figs 5–12). For the example simulation shown in Fig. 1, the fibre parameters are those of the GRIN fibre used in the experiment, and the initial pulse is chosen to be uniformly distributed into the first five modes, with identical phases in each mode. Simulations involving more and/or different modes show qualitatively similar results (Supplementary Figs 21 and 22), and the approximation made in restricting the number of modes for the analysis shown is made only to simplify the data and to allow efficient computation. We observe many simultaneous processes: an intense, Raman-shifting MM soliton (RS); a dispersive wave radiated by the pump at 850–1,000 nm (pump dispersive wave, PDW); and a series of sharp peaks (P) in both the visible and mid-infrared regions. As we will show in the following, by exploiting the spatial degrees of freedom, these effects can be controlled and enhanced by many orders of magnitude.

Although we use conventional terminology to describe the processes involved in our simulations and experiments, it is important to clarify how these effects differ from those observed in SMFs (Supplementary Fig. 12). The presence of many interacting modes implies that there are many more pathways to phase-match nonlinear wave-mixing processes, as each mode has a different dispersion relation $\beta_i(\omega)$. Because of this dispersive diversity and the fact that all modes are dissimilarly coupled through their spatial overlaps, propagation is much more complex than in SMF. Indeed, light in each mode can be affected in many different ways by light in other modes as a result of cross-phase modulation, four-wave mixing and Raman scattering. A prominent class of such effects comprises those associated with multimode solitons, where pulses in multiple spatial modes lock together into a single soliton entity. These new features, distinct from single-mode propagation, lead to the two key results of this work. First, because of the dispersive and mode-coupling diversity, nonlinear pulse propagation depends on the initial distribution of the optical field among the modes. Second, because nonlinear effects occur between modes, quantities like energy, phase and frequency are modified on an intermodal basis and therefore spatial nonlinear effects can be observed.

In the present experiments, pulses were launched from an amplified fibre laser at 1,550 nm (0.193 PHz), with a pulse duration of 500 fs, into an ~1 m GRIN fibre. The initial spatial condition was controlled by adjusting the position of the fibre relative to the launched beam (Supplementary Fig. 3). By adjusting the input conditions while viewing a given (output) measurement in real time, we observed, tuned and enhanced the same features observed in our

[1]School of Applied and Engineering Physics, Cornell University, Ithaca, New York 14853, USA. [2]CREOL, College of Optics and Photonics, University of Central Florida, Orlando, Florida 32816, USA. *e-mail: lgw32@cornell.edu

© 2015 Macmillan Publishers Limited. All rights reserved

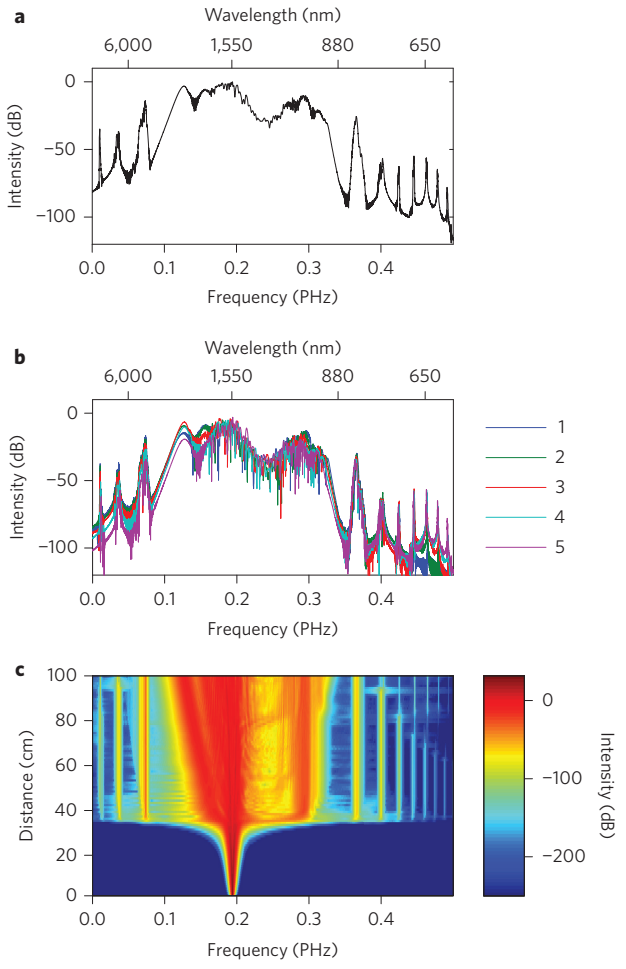

Figure 1 | Simulation results showing the spectral features of high-energy propagation in a multimode GRIN fibre. a, Total spectrum. **b**, Spectrum in each of the first five modes (sequentially dark blue, green, red, light blue and purple). **c**, Total spectrum evolution through the 1 m fibre. The mode-resolved temporal evolution and a larger version of **b** are presented in Supplementary Figs 1 and 2.

simulations. Figure 2a–e presents different spectra measured in the near- to mid-infared, while Fig. 2f–l shows the visible portion of the spectrum, with the corresponding final near-field beam profiles ('output beam profiles') shown to the right. Our results clearly indicate that by judiciously varying the initial spatial conditions one can greatly enhance the generation of either a dispersive wave radiated from multimode solitons at the 1,550 nm pump wavelength (PDW), Raman-shifted solitons (RS, in the lower panel a single soliton with energy above 40 nJ, centred above 2,200 nm), or both simultaneously. By placing a long-wavelength-pass filter after the fibre and optimizing the transmission, a single soliton is obtained at 2,100 nm, with a duration of 55 fs and energy >90 nJ (see spectrum before filtering in Fig. 2m and autocorrelation in Supplementary Fig. 4). These pulses are comparable in peak power to the best achieved to date by fibre sources at this wavelength[17].

Figure 2f–l presents example spectra in the visible portion of the spectrum. Due to the limited spectrometer dynamic range, some features saturate the detector. As a rough reference, however, note that the intensity of the PDW in each panel is approximately similar to that in the left and right panels. We often observe a strong peak at 516 nm (corresponding to third-harmonic generation (THG) of the pump) and various dispersive waves from Raman solitons (RSDW). In addition, the visible region is filled with a remarkable series of peaks (P). A series typically starts at roughly 832, 732 and 652 nm, followed by peaks of denser spacing that continue past the THG peak. These visible peaks agree well with the simulation results (Fig. 1). Surprisingly, the simulations suggest that the visible peaks are generated simultaneously with similar peaks in the infrared region near 3,800, 30,000 and 75,000 nm, in spite of the opacity of fused silica in the infrared. Although some features of these peaks are consistent over all conditions (for example, the location of the first few peaks and the spacing of the bluer peaks), their structure can change significantly depending on the energy and spatial initial conditions (Fig. 2f–l). This variation is also observed in simulations, which show that under a variety of initial excitations, the peaks appear to originate during the formation of a compressing multimode pulse which just precedes fission into multiple multimode solitons (Supplementary Movies 1 and 2). The peaks are observed only when third-order dispersion is included in the simulation, but do not require any other higher-order effects (Supplementary Discussion II and Supplementary Figs 12–20). The observations suggest a tentative hypothesis wherein the intense multimode pulse creates a nonlinear temporal cavity that resonantly amplifies parts of the continuum. Due to the presence of modal dispersion, the compressed pulse in the GRIN multimode fibre tends to be longer than the pulse in SMF, resulting in a smaller frequency spacing between peaks and allowing many peaks to be observed in the transparency range of the fibre. This process resembles those considered in works on analogue optical event horizons[18,19], but as the present multimode situation is considerably richer, more work will be required to confirm and develop this connection.

The observed diversity of outputs is due not only to the variety of excitation conditions, but also to the complexity of nonlinear interactions between modes. An equivalent view of this complexity is that nonlinear pulse propagation is inherently spatiotemporal. A particular example is presented in Fig. 3, where the near-field beam profile at the output of the fibre is shown for progressively higher input energies. Although the pulse has at most only a small fraction (<10%) of the critical power required for self-focusing, we initially observe an effect that bears a strong resemblance to the self-focusing of powerful beams in bulk media. Just as the spectral-temporal dynamics of one-dimensional single-mode solitons provide a framework to understand one-dimensional nonlinear effects—for example, supercontinuum generation, mode-locked lasers[20] and rogue waves[21]—the spatial-spectral-temporal dynamics of MM solitons[3–5,8,22] can provide a platform for understanding and in turn exploiting exploit three-dimensional nonlinear spatiotemporal processes. In MM GRIN fibres, the fundamental mode has the greatest intensity and overlap with all the other modes. It therefore has the greatest Raman coupling and typically the greatest net Raman gain. In GRIN Raman amplifiers, this causes the amplification of a fundamental mode beam by a multimode pump, termed 'Raman beam clean-up'[9,11,22,23]. In our experiments, this effect manifests as self-focusing as the extended high-order modes amplify lower-order modes. This occurs concomitantly with the compression, fission and self-frequency shift of MM solitons[22]. Soliton fission creates low-order-mode MM solitons that, for sufficient energy, shift beyond the spectral range of the camera (1,750 nm). They leave behind dispersive waves and MM solitons in higher-order modes, resulting in the speckling visible in the third image. Finally, vertical filaments grow from the speckled beam. We believe that the origin of the filamentation process is similar to that of transverse spatial hole burning in multimode laser cavities[24]. In the case described here, self-focusing leads to a local depletion of 1,550 nm pump light at the very centre of the fibre until, eventually, the available pump light and local intensity are too low for modes primarily centred there (that is, $m = 0$) to dominate the Raman gain competition. At this point, intensity spikes in the periphery

© 2015 Macmillan Publishers Limited. All rights reserved

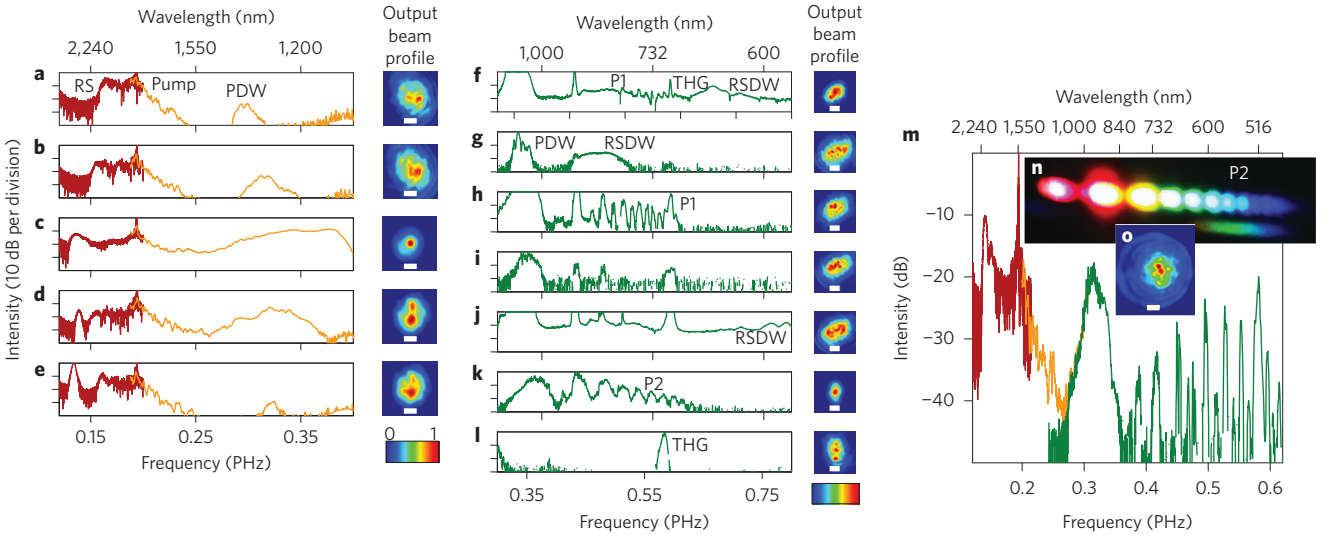

Figure 2 | Experimental results for optimizing effects in the spectral domain. Near- to mid-infrared spectra, with corresponding near-field beam profiles. **a**,**b**, Typical behaviour for increasing energy (120 nJ to 180 nJ, with the same initial spatial condition). **c**–**e**, By adjusting the initial spatial excitation, we optimize the spectral uniformity and bandwidth (**c**), the dispersive wave intensity (**d**) and the Raman soliton intensity (**e**) (the energy for each plot is ~150 nJ). **f**–**l**, Visible spectra (all ~150 nJ): typical result before adjustment (**f**), optimization of RSDW intensity (**g**), P1 intensity (**h**), the longest-wavelength peaks of P1 (**i**), RSDW frequency (**j**), P2 intensity (**k**) and THG intensity (**l**). **m**, Full spectrum for optimization of RS energy (total energy 250 nJ). **n**,**o**, Diffracted P2 photograph (**n**) and near-field beam profile (**o**) corresponding to **m**. The horizontal slant in **o** is due to an aberration of the imaging telescope. Scale bars: 17 μm.

of the fibre locally receive Raman gain, resulting in a multipeaked beam profile.

The results reported here could have important implications for short-pulse and broadband fibre sources and nonlinear fibre optics. Selectively optimizing a variety of effects highlights the potential role of a multimode fibre as a versatile light source, which may even be fine-tuned *in situ* for a given application. Considering also the enhanced energy capacity of multimode fibres, the results here demonstrate an important first step towards low-cost, low-maintenance, small-footprint, portable light sources to replace solid-state (for example, Ti:sapphire-based) sources as multipurpose tools in biology, chemistry and materials science. By using a spatial light modulator and multimode GRIN fibre in an adaptive optimization loop (a nonlinear extension of work on imaging through highly multimode fibres and scattering media[25]) a fibre laser may be capable of reaching many important combinations of pulse parameters. In multimode fibres made of fluoride or chalcogenide materials[26], tunable ultrafast mid-infrared light sources should be possible over an unprecedented bandwidth. Although we have not observed extremely high sensitivity to initial conditions or to fibre motion, the details of the output field do depend on the position of the fibre and on the exact alignment into the fibre. Such an adaptive loop would also be useful for ensuring environmental stability. In many applications, the non-Gaussian beam of many output states will not be especially limiting (most commercial fibre lasers are based on multimode fibres already, and even the most multimode features of the dispersed peaks in Fig. 2 are roughly Gaussian beams). Although considerable work will be required to determine the practical limits, input optimization can also be used to control the output spatial profile. For example, one can adjust the input

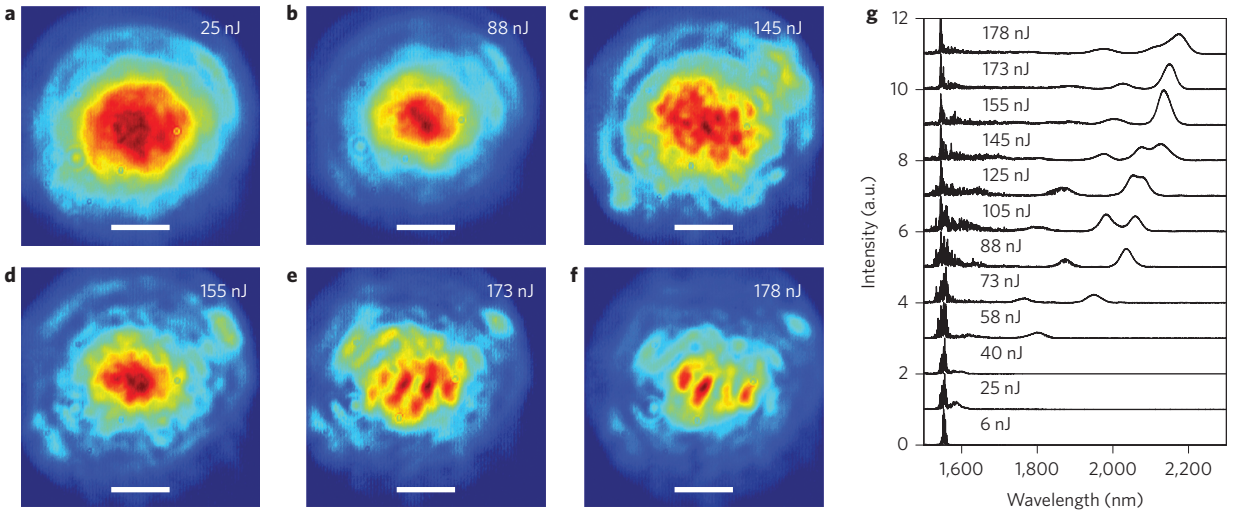

Figure 3 | Spatiotemporal dynamics in multimode GRIN fibre. a–**f**, Near-field beam images showing the self-focusing, speckling, refocusing and multiple filamentation as the energy of a launched pulse is increased. Scale bars: 17 μm. **g**, Corresponding spectra (linear scale) showing the formation of multimode Raman-shifting solitons, whose competitive formation dynamics can help explain the spatial observations.

© 2015 Macmillan Publishers Limited. All rights reserved

condition to optimize the beam quality or to achieve output Gaussian-like beams of various sizes. In addition to providing a degree of freedom for spatiotemporally and spectrally tailored light, spatial nonlinear effects could also prove useful for optical signal processing for space-division multiplexing[27,28].

Aside from applications, there are many directions for novel physics in nonlinear multimode fibres. For example, spatiotemporal multimode nonlinear dynamics are of considerable interest in the regime of optical wave turbulence[29]. These same processes can also manifest themselves in different ways in other types of multimode structures, such as step-index, multicore[30] and photonic crystal fibres. In such systems the modes may be heavily degenerate, or may be coupled due to a strong nonlinearity and broad bandwidth.

In summary, the rich nonlinear dynamics of multiple copropagating modes in multimode fibres offer a powerful degree of freedom for controlling an array of optical effects. In a multimode optical fibre, this control is readily accessed by adjusting the initial mode excitation conditions. The complex coupling between many spatial modes means that nonlinear effects are spatiotemporal. In all, the system has some similarities with both bulk media and single-mode waveguides, which have been extensively studied, but also provides many unique effects and opportunities that make it an important, new avenue in nonlinear optics. Spatiotemporal nonlinear dynamics in multimode systems may have important implications for fibre light sources that have higher power, broader bandwidth and greater tunability than single-mode sources. They may also be useful for optical information processing or coherent beam combining.

Methods

Simulations. Simulations to guide the experiments were conducted using the generalized multimode nonlinear Schrödinger equation[7] (GMM-NLSE, Supplementary equation (1) and Supplementary Discussion I) and a (2 + 1)-D generalized NLSE[22], with $n_2 = 2.3 \times 10^{-20}$ m^2 W^{-1} and with mode parameters and dispersion calculated assuming a Ge-doped fused-silica core as in ref. 6. The result shown in Fig. 1 used a GMM-NLSE including the effects of stimulated Raman scattering, dispersion up to third order, self-steepening, and loss (which is assumed to increase exponentially into the IR from 0.193 PHz/1,550 nm with a characteristic scale of 100 nm). Simulations including the additional effects of noise and spontaneous Raman scattering produced results similar to those of the more simplified model. For the simulation result shown in Fig. 1, we initialized simulations with 500 fs pulses at 0.193 PHz with equal energy and phase in each of the first five modes of the GRIN fibre used in the experiment ($m = 0$, or zero angular momentum modes). We assumed only a single linear polarization, which was justified by the short fibre and the use of the $m = 0$ modes (for details see Supplementary Discussion I). One of the simplest possible changes to the initial spatial condition, which can be efficiently modelled with only five modes, is changing the initial beam dimensions. Supplementary Figs 5–11 show the result of 50 cm of propagation for a beam waist from 30 to 3 μm. When more modes are considered, the details of the results are different but are qualitatively similar (Supplementary Figs 21 and 22). In the experiments, many more than the first five $m = 0$ modes may be relevant. There is therefore a larger dispersion relation diversity and more spatial degrees of freedom. Nonetheless, the simulations still show qualitatively the same phenomena, with the advantage of being significantly simpler to carry out and to plot.

Experiments. Pulses were coupled with up to 300 nJ energy, 400–500 fs duration and 1,550 nm wavelength into a GRIN fibre with a length of ~1 m using a three-axis translation stage and 6 cm lens (Supplementary Fig. 3). The fibre was a standard telecommunications product with a core diameter of 62.5 μm and 0.275 NA. The spectrum, which varies in space, was measured with defocused coupling into several different spectrometers. To confirm that this captured an overall average of the field, we compared the energy contained in the spectrum above 1,800 nm to the energy measured using a Ge window. As the latter acts as a spatially-indiscrimate long-pass filter, cutting on at 1,800 nm, and because its reflectivity and absorption spectrum are well known, it can be used to obtain an accurate measurement of the energy above 1,800 nm. The full-field autocorrelation[22] was measured using a two-photon absorption autocorrelator. The near-field beam profile was imaged onto an InGaAs camera. Although the beam was imaged to cover most of the pixels, the camera had a relatively modest 256 × 320 array size, and so we expected that some fine details of the beam profile were probably not captured. Furthermore, because the spatial phase evolves very rapidly in GRIN fibre, we expected that the measured beam profiles would show some averaging[22]. Mode-coupling effects due to bending and strain of the fibre were avoided by the use of a short fibre, primarily centralized launches and by holding the fibre nearly straight[6]. For the highest-order modes, mode coupling due to mechanical perturbations of the fibre was difficult to avoid. For results involving even the broadest distribution of modes, however, we typically observed minor changes to our measurements when the fibre was gently mechanically strained.

Received 7 January 2015; accepted 16 March 2015; published online 13 April 2015

References

1. Couairon, A. & Mysyrowicz, A. Femtosecond filamentation in transparent media. *Phys. Rep.* **441,** 47–189 (2007).
2. Eisenberg, H. *et al.* Kerr spatiotemporal self-focusing in a planar glass waveguide. *Phys. Rev. Lett.* **87,** 043902 (2001).
3. Hasegawa, A. Self-confinement of multimode optical pulse in a glass fiber. *Opt. Lett.* **5,** 416–417 (1980).
4. Crosignani, B. & Di Porto, P. Soliton propagation in multimode optical fibers. *Opt. Lett.* **6,** 329–330 (1981).
5. Yu, S. S., Chien, C.-H., Lai, Y. & Wang, J. Spatio-temporal solitary pulses in graded-index materials with Kerr nonlinearity. *Opt. Commun.* **119,** 167–170 (1995).
6. Mafi, A. Pulse propagation in a short nonlinear graded-index multimode optical fiber. *J. Lightw. Technol.* **30,** 2803–2811 (2012).
7. Poletti, F. & Horak, P. Description of ultrashort pulse propagation in multimode optical fibers. *J. Opt. Soc. Am. B* **25,** 1645–1654 (2008).
8. Kivshar, Y. S. & Agrawal, G. P. *Optical Solitons: From Fibers to Photonic Crystals* 1st edn (Academic, 2003).
9. Baldeck, P. L., Raccah, F. & Alfano, R. R. Observation of self-focusing in optical fibers with picosecond pulses. *Opt. Lett.* **12,** 588–589 (1987).
10. Grudinin, A. B., Dianov, E. M., Korbkin, D. V., Prokhorov, A. M. & Khaĭdarov, D. V. Nonlinear mode coupling in multimode optical fibers; excitation of femtosecond-range stimulated-Raman-scattering solitons. *J. Exp. Theor. Phys. Lett.* **47,** 356–359 (1988).
11. Pourbeyram, H., Agrawal, G. P. & Mafi, A. Stimulated Raman scattering cascade spanning the wavelength range of 523 to 1750 nm using a graded-index multimode optical fiber. *Appl. Phys. Lett.* **102,** 201107 (2013).
12. Stolen, R. H. Phase-matched three-wave mixing in silica fiber optical waveguides. *Appl. Phys. Lett.* **24,** 308 (1974).
13. Cheng, J. *et al.* Intermodal Čerenkov radiation in a higher-order-mode fiber. *Opt. Lett.* **37,** 4410–4412 (2012).
14. Ramsay, J. *et al.* Generation of infrared supercontinuum radiation: spatial mode dispersion and higher-order mode propagation in ZBLAN step-index fibers. *Opt. Express* **21,** 10764–10771 (2013).
15. Tani, F., Travers, J. C. & Russell, P. St. J. Multimode ultrafast nonlinear optics in optical waveguides: numerical modeling and experiments in kagomé photonic-crystal fiber. *J. Opt. Soc. Am. B* **31,** 311–320 (2014).
16. Russell, P. St. J., Hölzer, P., Chang, W., Abdolvand, A. & Travers, J. C. Hollow-core photonic crystal fibres for gas-based nonlinear optics. *Nature Photon.* **8,** 278–286 (2014).
17. Sims, R. A., Kadwani, P., Shah, A. S. L. & Richardson, M. 1 μJ, sub-500 fs chirped pulse amplification in a Tm-doped fiber system. *Opt. Lett.* **38,** 121–123 (2013).
18. Philbin, T. G. *et al.* Fiber-optical analog of the event horizon. *Science* **319,** 1367–1370 (2008).
19. Webb, K. E. *et al.* Nonlinear optics of fibre event horizons. *Nature Commun.* **5,** 4969 (2014).
20. Mollenauer, L. F. & Stolen, R. H. The soliton laser. *Opt. Lett.* **9,** 13–15 (1984).
21. Dudley, J. M., Dias, F., Erkintalo, M. & Genty, G. Instabilities, breathers and rogue waves in optics. *Nature Photon.* **8,** 755–764 (2014).
22. Wright, L. G., Renninger, W. H., Christodoulides, D. N. & Wise, F. W. Spatiotemporal dynamics of multimode optical solitons. *Opt. Express* **23,** 3492–3506 (2015).
23. Goldhar, J. & Murray, J. Intensity averaging and four-wave mixing in Raman amplifiers. *IEEE J. Quantum Electron.* **18,** 399–409 (1982).
24. Sun, L. & Marciante, J. R. Filamentation analysis in large-mode-area fiber lasers. *J. Opt. Soc. Am. B* **24,** 2321–2326 (2007).
25. Mosk, A. P., Lagendijk, A., Lerosey, G. & Fink, M. Controlling waves in space and time for imaging and focusing in complex media. *Nature Photon.* **6,** 283–292 (2012).
26. Petersen, C. R. *et al.* Mid-infrared supercontinuum covering the 1.4–13.3 μm molecular fingerprint region using ultra-high NA chalcogenide step-index fibre. *Nature Photon.* **8,** 830–834 (2014).
27. Winzer, P. J. Optical networking beyond WDM. *IEEE Photon. J.* **4,** 647–651 (2012).
28. Richardson, D. J., Fini, J. M. & Nelson, L. E. Space-division multiplexing in optical fibres. *Nature Photon.* **7,** 354–362 (2013).

© 2015 Macmillan Publishers Limited. All rights reserved

29. Picozzi, A. *et al.* Optical wave turbulence: towards a unified nonequilibrium thermodynamic formulation of statistical nonlinear optics. *Phys. Rep.* **542,** 1–132 (2014).
30. Fang, X. *et al.* Multiwatt octave-spanning supercontinuum generation in multicore photonic-crystal fiber. *Opt. Lett.* **37,** 2292–2294 (2012).

Acknowledgements

Portions of this work were funded by the Office of Naval Research (grant no. N00014-13-1-0649). L.G.W. acknowledges support from NSERC and thanks E. Lamb for taking the photograph in Fig. 2n. The authors thank C. Xu for the loan of the laser used in the experiments and W. Renninger and A. Mafi for discussions.

Author contributions

L.G.W. performed experiments and simulations. L.G.W., D.N.C. and F.W.W. wrote the manuscript.

Additional information

Supplementary information is available in the online version of the paper. Reprints and permissions information is available online at www.nature.com/reprints. Correspondence and requests for materials should be addressed to L.G.W.

Competing financial interests

The authors declare no competing financial interests.

© 2015 Macmillan Publishers Limited. All rights reserved